J. Fluid Mech. (1989), *vol.* 208, *pp.* 375–393
Printed in Great Britain

Critical geometry of oscillating bluff bodies

By YASUHARU NAKAMURA AND KATSUYA HIRATA
Research Institute for Applied Mechanics, Kyushu University, Kasuga 816, Japan

(Received 6 July 1988 and in revised form 25 April 1989)

Measurements are presented of the mean pressures around rectangular and D-section cylinders, with a flat front face normal to the flow, forced to oscillate transversely at an amplitude of 10% of the length of the front face. The ratio of depth (streamwise dimension) to height (cross-stream dimension) of the cross-section ranges from 0.2 to 1.0 for rectangular cylinders and from 0.5 to 1.5 for D-section cylinders. The range of reduced velocities investigated, 3 to 11, includes the vortex-resonance region. When increasing the depth, an oscillating bluff cylinder shows a critical depth where base suction attains a peak. The value of a critical depth is lowered with decreasing reduced velocity. In particular, an extraordinarily low critical depth with a very high base suction is obtained on cylinders oscillating at vortex resonance. For cylinders with depths beyond the critical, a reattachment-type pressure distribution is established on the afterbody due to the shear-layer/edge direct interaction. The shear-layer/edge direct interaction can also occur on oscillating cylinders with a fixed splitter plate. At low reduced velocities, the reattachment-type pressure distributions on cylinders with and without a splitter plate are similar except for the mean level. A remark is made on the critical geometry of bluff bodies under various flow conditions.

1. Introduction

Recent development in wind engineering has greatly renewed interest in the separated flow past bluff bodies (see, for example, Bearman 1984; Nakamura 1988). The flow around tall buildings and long suspension bridges exposed to the wind is highly complicated, and they are susceptible to wind-induced oscillations of various kinds. A detailed analysis of the physical processes involved in bluff-body flow is required to predict precisely the wind loads experienced by such buildings and structures.

One of the most interesting aspects of the problem is the effect of body oscillation on the (time) mean and unsteady bluff-body flows, where the complex interaction between the body oscillation and the formation and shedding of vortices plays a central part. In this paper the problem of the effect of body oscillation on the mean bluff-body flow is considered. It has a close link with the effect of the free-stream turbulence on the mean bluff-body flow (e.g. Nakamura & Ohya 1984), although body oscillation normally generates two-dimensional velocity fluctuations and turbulence essentially consists of three-dimensional velocity fluctuations.

It has been known that the (mean) base pressure of a bluff body is very sensitive to body oscillation, and it is also strongly dependent on the afterbody shape. For example, the base pressures of a normal flat plate, a circular cylinder and a D-section cylinder (with a depth-to-height ratio of 0.5 in the present terminology), subject to transverse oscillation, are decreased considerably at vortex resonance, where the

body frequency is equal to the vortex-shedding frequency for a stationary cylinder, while those of a square-section and a triangular cylinder with a vertex pointing downstream are no lower than the values measured on stationary cylinders (Bearman & Davies 1977; Bearman & Obasaju 1982). On the other hand, the base pressure of a rectangular cylinder with a depth-to-height ratio of 0.4 shows a critical minimum at vortex resonance (Mizota 1984). The mechanisms by which such complicated base-pressure variations are produced remain unclear. The present investigation is concerned with the mean flow past rectangular and D-section cylinders with variable afterbody lengths that are subject to transverse oscillation. The principal aim of the present investigation is to correlate existing knowledge on mean bluff-body flow more systematically.

2. Some related topics on bluff-body flow

2.1. *Critical geometry of stationary bluff cylinders*

The work of Nakaguchi, Hashimoto & Muto (1968) on stationary rectangular cylinders showed that, as the cylinder depth is increased from zero, base pressure decreases rapidly to a critical minimum at a depth just beyond about 0.6 times the height. Bearman & Trueman (1972) argued that the decrease in base pressure for cylinders with depths below the critical is associated with an increased curvature of the shear layer in roll-up as a result of a reduced base-cavity size. They also suggested that the increase in base pressure for cylinders with depths beyond the critical is associated with vortices being forced to form further downstream as a result of the influence of the rear corners.

The influence of the rear corner on the shear layer just mentioned is hereinafter referred to as the shear-layer/edge direct interaction. Nakamura & Tomonari (1981) showed that the shear-layer/edge direct interaction, the final stage of which is reattachment of the shear layer on the side face, yields a reattachment-type pressure distribution on the side face that is characterized by a low-pressure plateau followed by recovery to some high pressure. When a cylinder with a depth beyond the critical is at a small positive (clockwise) incidence, it experiences a downward load due to the pressure difference between the upper and lower side faces that is caused by the shear-layer/edge direct interaction. This is the reason why aeroelastic galloping can occur for rectangular cylinders with depths beyond the critical (Nakamura & Tomonari 1977, 1981). Laneville and his associates (Da Matha Sant'Anna *et al.* 1987) also discussed the pressure-recovery characteristics of rectangular cylinders.

2.2. *The effects of body oscillation on bluff-body flow*

It will be useful here to review the overall effects of body oscillation on the flow past a bluff body (Nakamura & Matsukawa 1987). The flow past an oscillating bluff body has two dominant frequency components; the frequency of body oscillation f_y and the frequency of natural vortex shedding f_v (natural vortex-shedding frequency refers to the frequency that would be obtained on a stationary cylinder under similar flow conditions).

The flow with the body frequency f_y consists of two main parts. One is the flow linked directly with the acceleration of the body, and the other is the flow responding to the continual variation of the angle of incidence of the body. The flow linked with the body acceleration may be dominant at low reduced velocities (see next section for the definition), but it is relatively insignificant for bluff bodies with short afterbodies.

The variation of the angle of incidence produces undulation of the wake, the wavelength of which is progressively shortened with decreasing reduced velocity. Wake undulation can manifest itself as motion-dependent vortices when the reduced velocity is low and the amplitude of the imposed body oscillation is large. However, the influence of the imposed body oscillation is present as wake undulation at any reduced velocity whether or not it manifests itself as motion-dependent vortices.

When the frequency of the imposed body oscillation approaches that of natural vortex shedding, a strong resonant interaction can occur between wake undulation and natural vortex shedding. The flow response at vortex resonance is restricted to a narrow range of reduced velocity, but it can create enormous changes in both steady and unsteady flow characteristics. For example, unsteady pressures and lift force exhibit typical linear resonance characteristics, i.e. a sharp peak in amplitude with an abrupt phase change at vortex resonance. For large amplitudes of body oscillation, the vortex-shedding frequency is locked-in to the body frequency. Improved spanwise correlation in vortex shedding is also characteristic of an oscillating bluff body. Since vortex shedding is a strongly nonlinear phenomenon, resonant interaction between vortex shedding and the imposed body oscillation can vitally influence the time-mean flow.

On this basis three distinct flow ranges of interest can be identified: the high-speed range where $f_y \ll f_v$, the range of vortex resonance where $f_y \approx f_v$, and the low-speed range where $f_y \gg f_v$.

3. Experimental arrangements

The experiments were conducted in a low-speed wind tunnel with a rectangular working section 3 m high, 0.7 m wide and 2 m long. The models used in the present experiment were rectangular and D-section cylinders. As is shown in figure 1, the cross-section of the D-section cylinders, as referred to here, was a rectangular–semicircle combination. The height h of the model was constant and equal to 15 cm, while the depth d varied widely. The depth-to-height ratio thus obtained was $d/h = 0.2$ to 1.0 for rectangular cylinders, and $d/h = 0.5$ to 1.5 for D-section ones. The model had 45 cm ($= 3\,h$) square end plates with a separation of 65 cm ($= 4.3\,h$) and it was mounted horizontally in the working section with a flat face normal to the flow.

The surface static pressures around the model were measured by using pressure taps of 0.3 mm diameter, and the wake static pressures along the model centreline were measured by using a long pressure tube of 2 mm diameter, which had four equally spaced holes of 0.3 mm diameter on its circumference. The pressure was determined with a calibrated inductance-type pressure transducer, and the mean pressure p is presented in the form of a pressure coefficient $C_p = (p-p_0)/(\frac{1}{2}\rho U^2)$, where p_0, ρ, and U are the mean static pressure, the air density and the velocity of the free stream respectively. A constant-temperature hot-wire anemometer was used to measure fluctuating flow velocities. A hot-wire probe was placed $1\,h$ down and $1.5\,h$ behind the front corner of the model.

The model was forced to oscillate transverse to the flow at a constant frequency of $f_y = 3$ or 6 Hz (mostly 6 Hz) with an amplitude of 1.5 cm ($= 0.1\,h$) by using an electro-mechanical vibrator. The flow velocity was varied from about $U = 2.5$ to 10.0 ms^{-1} so that the reduced velocity, defined by $\bar{U} = U/(f_y h)$, ranged from about 2.8 to 11.1, including the vortex-resonance velocity $\bar{U}_r$. $\bar{U}_r$ is given by $\bar{U}_r = U/(f_v h)$,

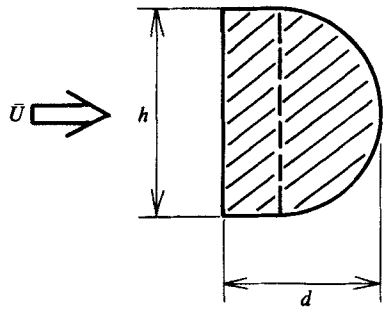

FIGURE 1. D-section model.

and hence is equal to the inverse of the Strouhal number for a stationary cylinder. The range of the Reynolds number, which is based on the model height h, was about $(2.5 \text{ to } 10) \times 10^4$.

In some cases a wool-tuft test was made to see whether or not the flow reattached on the afterbody of the model. An experiment was added using D-section cylinders with a long splitter plate placed downstream and fixed relative to the tunnel walls. The splitter plate was $11.3\,h$ in length and $0.07\,h$ in thickness, and the gap between the model and the splitter plate was about $0.1\,h$.

4. Experimental results

4.1. *Pressure distributions around a rectangular and a D-section cylinder*

Table 1 shows the Strouhal number S, based on h, and the corresponding vortex-resonance velocity $\bar{U}_r (= 1/S)$ for stationary rectangular and D-section cylinders, which were determined by use of a hot-wire anemometer. Initial measurements on stationary cylinders showed that the base pressure along the cylinder span was reasonably uniform in agreement with a previous similar experiment (Nakamura & Matsukawa 1987). Figure 2 shows pressure distributions around a rectangular cylinder with $d/h = 0.4$, together with those along the wake centreline, for four values of the reduced velocity, stationary, $\bar{U} = 8.9$, $7.2\,(= 1.11\bar{U}_r)$ and 3.9, while figure 3 shows pressure distributions around a D-section cylinder with $d/h = 0.5$. The front-face pressure distributions of a rectangular and a D-section cylinder showed nothing unusual. They were almost independent of changing both the depth and the reduced velocity, and, therefore, any changes in drag will be reflected by changes in base pressure. Figure 2 shows that the pressure on the stationary cylinder was reasonably uniform over the afterbody, whereas the pressure along the wake centreline decreased rapidly owing to vortex formation before recovering towards the free stream value. One of the interesting features shown in figure 3 is that the pressure on the stationary cylinder was not uniform but decreased considerably along the afterbody from the separation point to the base. The results for oscillating cylinders are the main topics of this investigation and will be discussed in later sections.

4.2. *The effects of blockage, end plates and the Reynolds number*

In an experiment using a sectional model with end plates the combined blockage and end effects should be considered. Generally, the two effects have opposite signs; the former decreases the base pressure of a bluff body whereas the latter increases it.

			Rectangular cylinders				
d/h	0.2	0.3	0.4	0.5	0.6	0.8	1.0
S	0.156	0.156	0.154	0.147	0.143	0.135	0.127
$\bar{U}_r$	6.4	6.4	6.5	6.8	7.0	7.4	7.9
			D-section cylinders				
d/h	0.5	0.63	0.7	0.77	0.83	0.9	1.0
S	0.149	0.145	0.135	0.132	0.128	0.125	0.123
$\bar{U}_r$	6.7	6.9	7.4	7.6	7.8	8.0	8.1

TABLE 1. Strouhal number S and vortex-resonance velocity $\bar{U}_r$ ($= 1/S$) for stationary rectangular and D-section cylinders

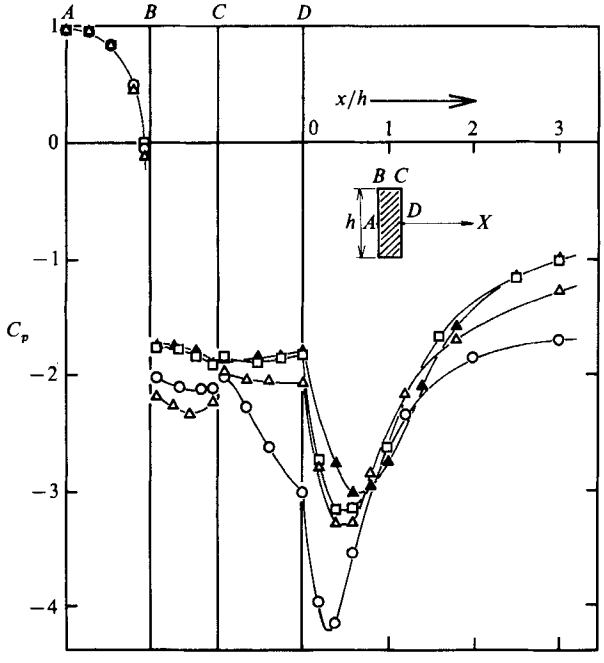

FIGURE 2. Pressure distribution around and behind a rectangular cylinder with $d/h = 0.4$. ▲, stationary; □, $\bar{U} = 8.9$; ○, 7.2 ($= 1.1\,\bar{U}_r$); △, 3.9.

In the present experiment the blockage ratio was as large as 5% and the size of the end plates used was relatively small so that their effects may be considerable. However, none of the results presented have been corrected for these two effects since there is no method of correction available for measurements made with an oscillating bluff body.

Figure 4 shows the base-suction coefficient $-C_{pb}$ of a stationary D-section cylinder plotted against depth-to-height ratio d/h for three different values of the Reynolds number. The results indicate that the effect of the Reynolds number was fairly considerable, and increasing Reynolds number produced increasing base suction for a range of d/h from 0.5 to 1.1. A similar, though relatively small, effect of the Reynolds number was observed on the base-suction coefficient of a stationary rectangular cylinder.

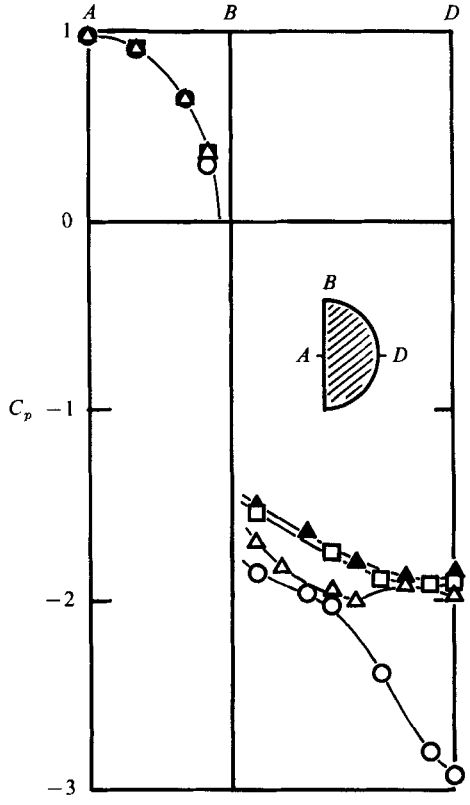

FIGURE 3. Pressure distributions around a D-section cylinder with $d/h = 0.5$. ▲, stationary; □, $\bar{U} = 8.9$; ○, 7.2 ($= 1.1\,\bar{U}_r$); △, 3.9.

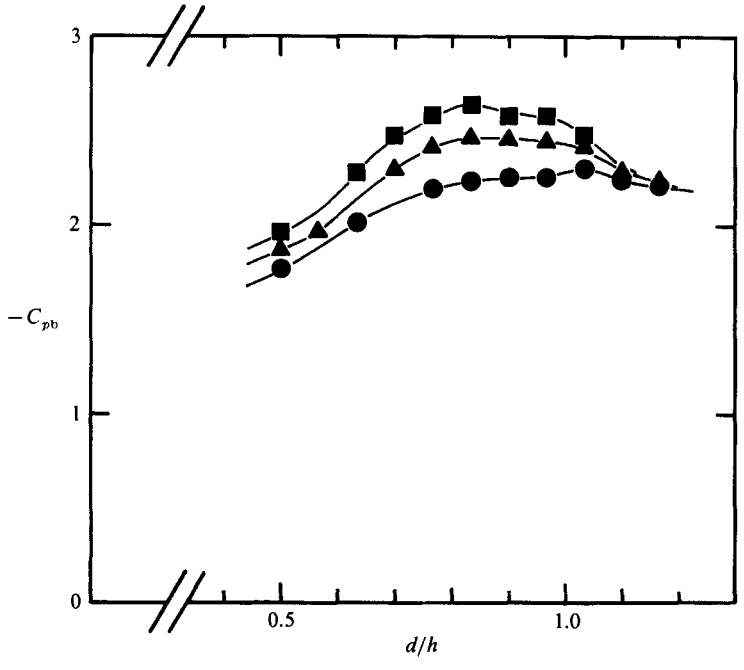

FIGURE 4. Effect of the Reynolds number on the base-suction coefficients of stationary D-section cylinders. ●, $Re = 0.3 \times 10^5$; ▲, 0.8×10^5; ■, 1.2×10^5.

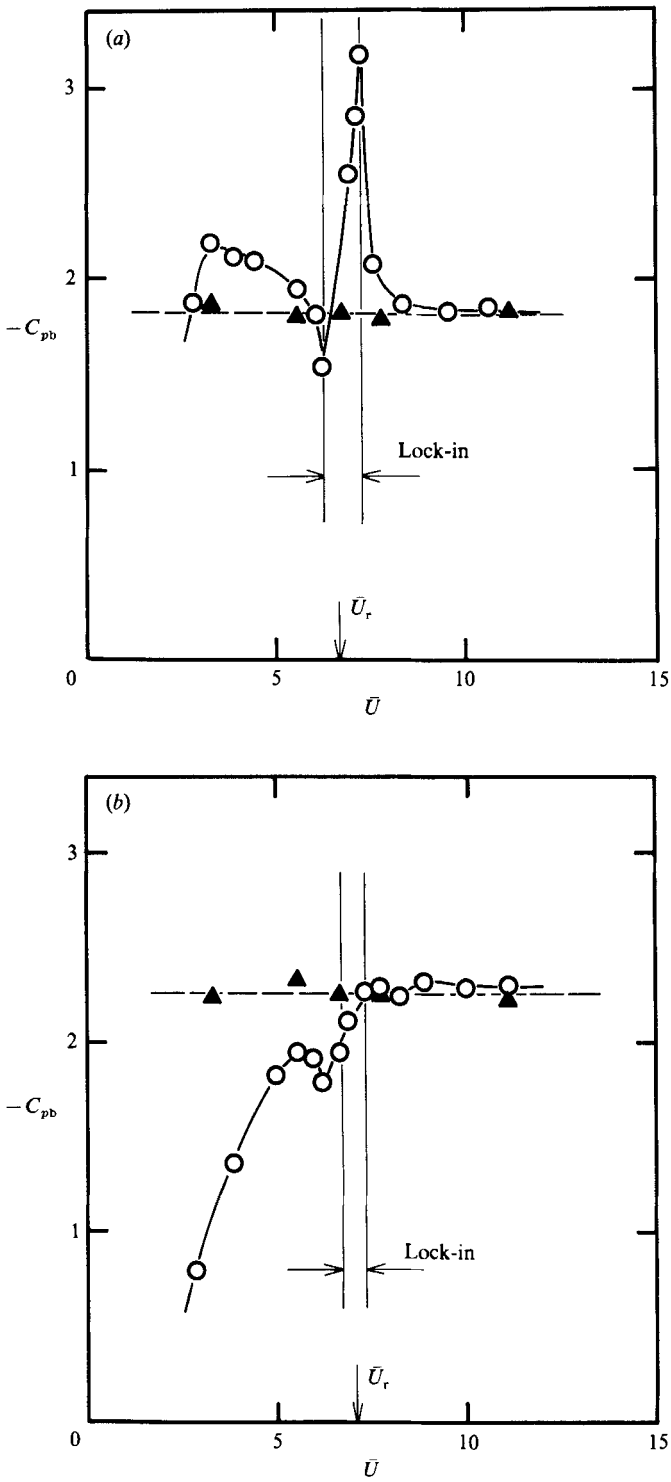

FIGURE 5(*a*, *b*). For caption see page 383.

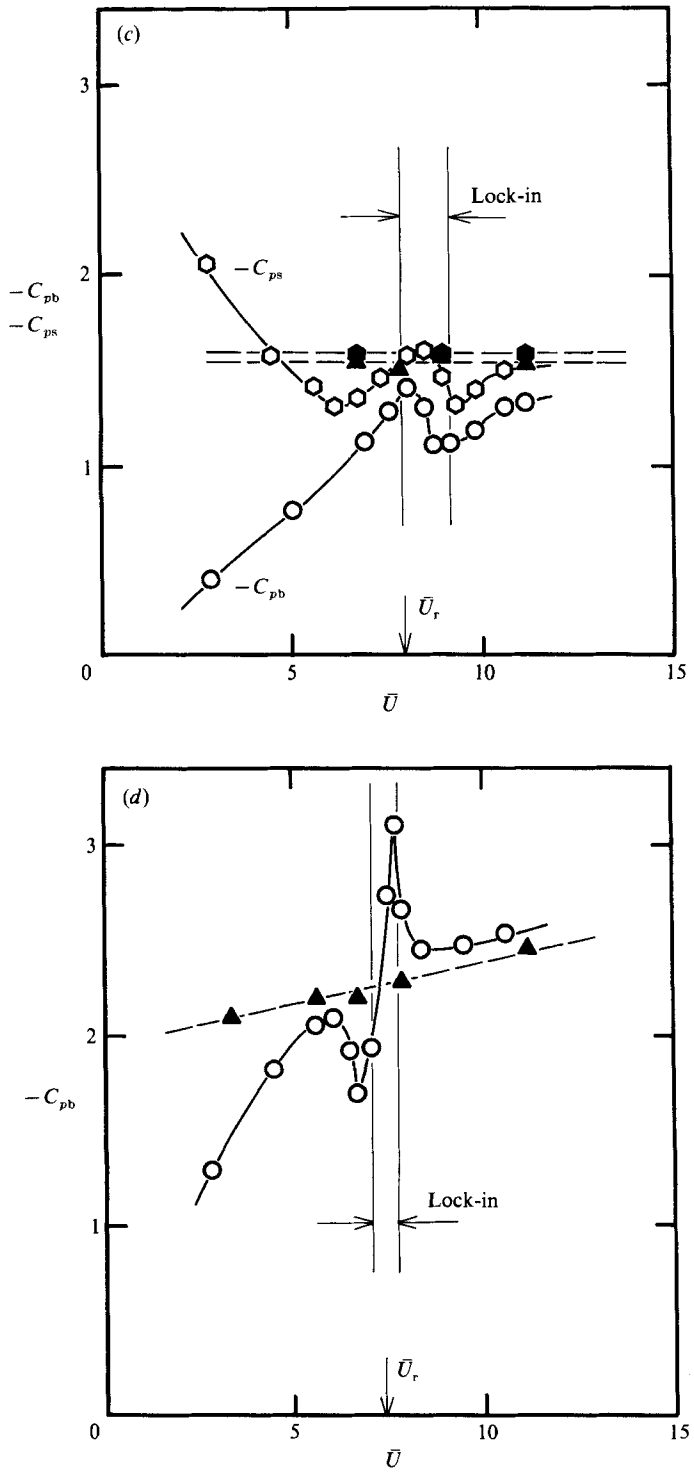

FIGURE 5(*c*, *d*). For caption see facing page.

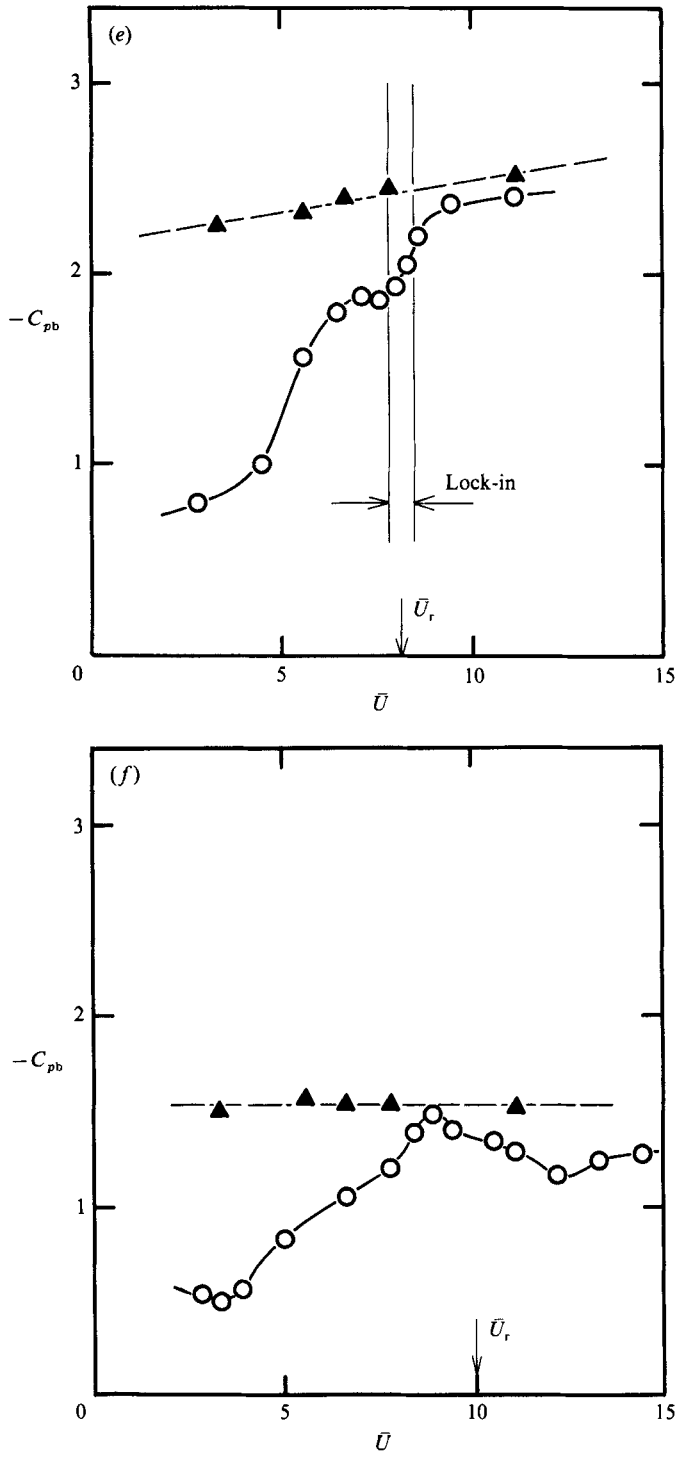

FIGURE 5. Base-suction coefficient versus reduced velocity for oscillating rectangular and D-section cylinders. Black symbols are for stationary cylinders. (*c*) includes the pressure coefficient at separation C_{ps}. (*a*) Rectangular cylinder with $d/h = 0.4$. (*b*) Rectangular cylinder with $d/h = 0.6$. (*c*) Rectangular cylinder with $d/h = 1.0$. (*d*) D-section cylinder with $d/h = 0.5$. (*e*) D-section cylinder with $d/h = 1.0$. (*f*) D-section cylinder with $d/h = 1.5$.

4.3. *The variation of the base-suction coefficient with reduced velocity*

In general the base-suction coefficient of an oscillating bluff body is dependent on the cross-section geometry, the reduced velocity and the reduced amplitude of oscillation, i.e. the amplitude relative to the body size ($= h$). As was mentioned earlier, the reduced amplitude of oscillation was constant throughout the experiment and equal to 0.1.

Figure 5 shows base-suction coefficients plotted against reduced velocity for a selection of rectangular and D-section cylinders. The base-suction coefficients on stationary cylinders were obtained over a range of the flow velocity tested. These are plotted in figure 5 with reduced velocities having a nominal value of frequency of 3 or 6 Hz. Because of the Reynolds-number effect (figure 4), they are more or less increased with reduced velocity. Although the base-suction coefficient varies in a very complicated way both with the reduced velocity and with the depth-to-height ratio, there is a close similarity in the base-suction characteristics between rectangular and D-section cylinders. The results for the base-suction coefficient of the square-section cylinder shown in figure 5(*c*) are in general agreement with those obtained by Bearman & Obasaju (1982). A rather significant difference between the two measurements is found in the range of frequency lock-in. Our lower end of lock-in, which was determined from the measurement of the fluctuating velocities in the wake, is close to the vortex-resonance velocity and somewhat higher than the value of Bearman & Obasaju, which was determined by the measurement of the fluctuating side-face pressures. Figure 5(*c*) also includes the results for the suction coefficient at separation $-C_{ps}$ measured at a position $0.05\,h$ downstream of the front corner.

5. Further experimental results and discussions

5.1. *Critical geometry of oscillating rectangular and D-section cylinders*

Figure 6 shows base-suction coefficients of rectangular cylinders plotted against depth-to-height ratio for various values of the reduced velocity. It can be seen that there is a critical depth showing a peak base suction at each reduced velocity. The value of a critical depth is lowered with decreasing reduced velocity. In particular, the critical depth at vortex resonance shows an extraordinarily low value of about 0.4 with a very high base suction, which is in agreement with Mizota (1984). Figure 7 shows similar results for D-section cylinders where the critical depth at vortex resonance is found to be equal to about $d/h = 0.7$. For low reduced velocities, say, $\bar{U} = 4.0$, there is no critical depth since the base suction is decreased progressively with increasing d/h from 0.5.

A comment is necessary on the critical depth at vortex resonance. In the vortex-resonance range a conventional plot of $-C_{pb}$ with a given value of $\bar{U}$ may not be practical since, as is seen in figure 5(*a*, *d*), the base-suction coefficient often varies very rapidly in this narrow range. We have instead plotted peak values of the base-suction coefficient. The reduced velocity at which a peak base suction occurred was not exactly equal to the vortex-resonance velocity but, for short cylinders, slightly higher depending on the amplitude of the imposed oscillation, and very close to the upper end of lock-in obtained for fluctuating flow velocities. It is conveniently referred to as the vortex-resonance velocity in figures 6 and 7. Figure 8 shows a plot of the critical depth against reduced velocity for rectangular and D-section cylinders along with that of the vortex-resonance velocity.

Critical depth may be dependent on the amplitude of body oscillation. Mizota

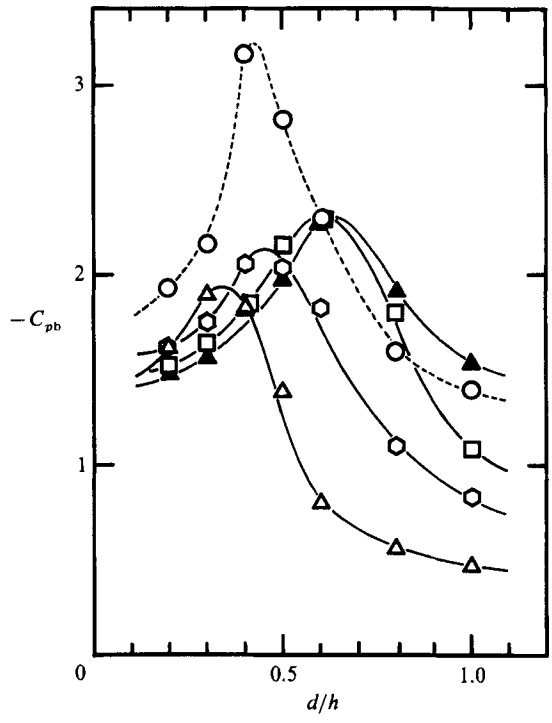

FIGURE 6. Base-suction coefficient versus d/h for oscillating rectangular cylinders. ▲, stationary; □, $\bar{U} = 8.9$; ○, $\bar{U}_r$; ⬡, 5; △, 2.8.

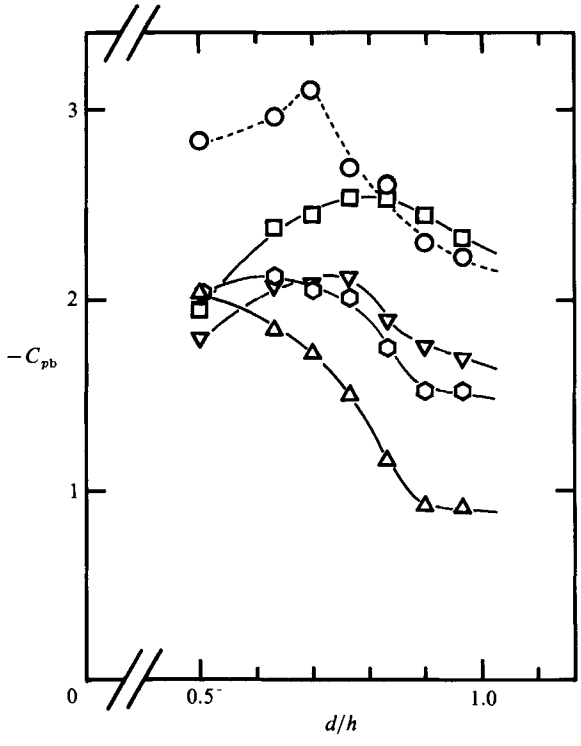

FIGURE 7. Base-suction coefficient versus d/h for oscillating D-section cylinders. □, $\bar{U} = 9$; ○, $\bar{U}_r$; ▽, 6; ⬡, 5.5; △, 4.

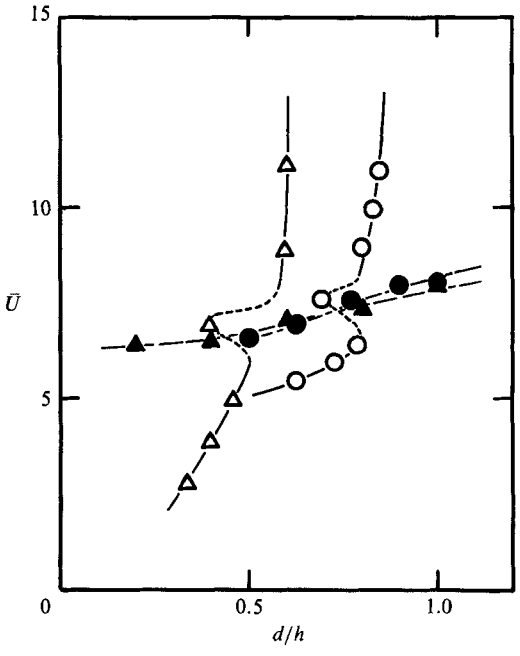

FIGURE 8. Critical geometry as a function of $\bar{U}$ and d/h. White symbols are for the critical depth, and black symbols are for the vortex-resonance velocity. △, ▲, rectangular cylinder; ○, ●, D-section cylinder.

(1984) conducted an experiment on rectangular cylinders oscillating at vortex resonance, where the reduced amplitude of oscillation was varied from 0.1 to 0.025. He found that the value of the critical depth remained unchanged and equal to $d/h = 0.4$ with decreasing oscillation amplitude, although the value of the peak base suction was progressively lowered and approached that corresponding to the stationary cylinder.

5.2. *The effect of wake undulation on bluff-body mean flow*

We consider the flow past an elongated bluff body where the separation bubble is formed on the side face downstream of the separation point. Nakamura & Ozono (1987) recently conducted an experiment on a separated-and-reattaching flow past a flat plate using an oscillating leading-edge spoiler and showed that the effect of spoiler oscillation is substantial and the separation bubble is progressively shortened with decreasing reduced velocity. The mechanism by which the separation bubble is shortened is that the Reynolds stresses in the turbulent shear layer are enhanced greatly by the wake undulation (or equivalently by the motion-dependent vortices), generated by the spoiler oscillation, to cause the shear layer to reattach earlier on the side face. We can assume that the same mechanism, enhanced Reynolds stresses in the undulated turbulent shear layer, could work for short bluff bodies where there is no flow reattachment. This can explain the present results that the critical depth is lowered progressively with decreasing reduced velocity except for the vortex-resonance range.

5.3. *Reattachment-type pressure distributions on oscillating cylinders*

As mentioned earlier, the shear-layer/edge direct interaction produces a reattachment-type pressure distribution on a stationary bluff cylinder (Nakamura & Tomonari 1981). It will be interesting to see how this concept applies to oscillating bluff cylinders. The problem was examined separately for the three different ranges of reduced velocity. The results for the high-speed range are not shown here, however, since they were not much different from those on stationary cylinders.

Figure 9 shows pressure distributions on four rectangular cylinders with different depths oscillating at vortex resonance. As can be seen, the side-face pressure distributions on cylinders with $d/h = 0.3$ and 0.4 are reasonably uniform whereas a reattachment-type pressure distribution can be identified on the side faces of cylinders with $d/h = 0.5$ and 0.6. We conclude therefore that when increasing the depth while keeping vortex resonance, a reattachment-type pressure distribution manifests itself at the critical depth, i.e. at a rectangular cylinder with $d/h = 0.4$. It should be noted that the flow has not yet reattached on the side face at the critical depth. The wool-tuft test indicated no sign of steady reattachment on a rectangular cylinder with $d/h = 0.8$ at reduced velocities down to $\bar{U} = 3.9$.

Figure 10 shows similar results for D-section cylinders. In this case, a reattachment-type pressure distribution is less easily identified. However, a local pressure recovery is seen during a large pressure drop towards the base for cylinders with $d/h = 0.83$ and 0.9 so that the conclusion remains the same as for rectangular cylinders.

As Bearman & Trueman (1972) discussed, there is a complicated interplay among the vorticity that is being shed from a bluff body, the base pressure and the downstream vortex formation. In figure 11 attention is paid to the base pressure C_{pb}, the minimum pressure in the wake C_{pw} and the pressure at separation C_{ps} to see how these three are varied with d/h for rectangular cylinders oscillating at vortex resonance (figure 11*a*) and at $\bar{U} = 3.9$ (figure 11*b*).

As is expected, the variation of $-C_{pb}$ with d/h in figure 11(*a*) is in line with that of $-C_{pw}$. It is seen that this is also true for $-C_{ps}$. In particular, the decrease in $-C_{ps}$ beginning at the critical depth indicates that there is substantial feedback control of the vortex formation over the flow at separation. However, it is interesting that the decrease in $-C_{ps}$ beginning at the critical depth is considerably smaller than that in $-C_{pb}$. If we define gross pressure recovery by $C_{pb}-C_{ps}$, it increases with d/h for cylinders with depths beyond the critical. Namely, a reattachment-type pressure distribution has been established on cylinders with depths beyond the critical. Although the gross pressure recovery is negative for d/h between the critical and $d/h = 0.7$, approximately, there is a significantly positive local pressure recovery on the side face, as is exemplified in figure 9 for cylinders with $d/h = 0.5$ and 0.6.

Figure 5(*a*, *d*) shows that a short bluff cylinder has a peak in base suction at a reduced velocity much lower than the vortex-resonance velocity. It was found, as expected, that the values of d/h and $\bar{U}$ at which this peak occurred collapsed on the curve of the critical depth given in figure 8.

Figure 5(*d*) indicates that the value of reduced velocity at which the D-section cylinder with $d/h = 0.7$ becomes critical is equal to $\bar{U} = 5.8$. Figure 12 shows pressure distributions on the same cylinder corresponding to four different values of reduced velocity. At the lowest reduced velocity, equal to $\bar{U} = 3.9$, much lower than the critical, a reattachment-type pressure distribution caused by the shear-layer/edge direct interaction is seen. With increasing reduced velocity, the interaction is

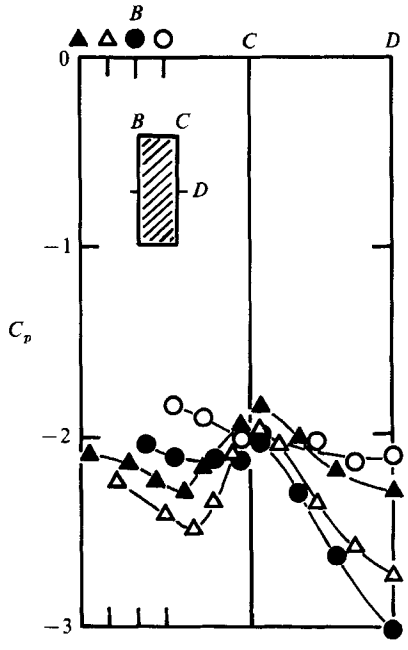

FIGURE 9. Pressure distributions around rectangular cylinders oscillating at vortex resonance. ○, $d/h = 0.3$; ●, 0.4; △, 0.5; ▲, 0.6.

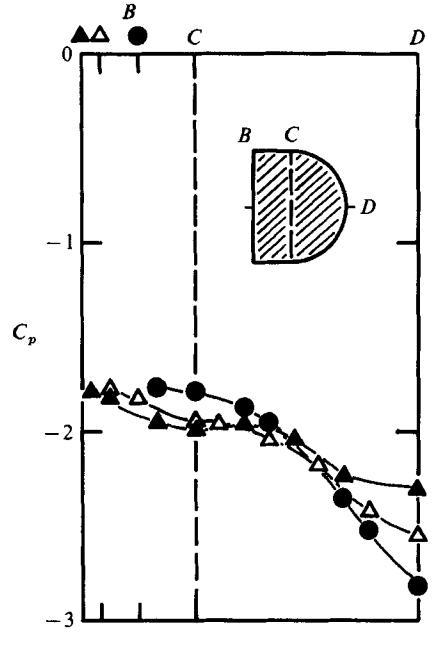

FIGURE 10. Pressure distributions around D-section cylinders oscillating at vortex resonance. ●, $d/h = 0.7$; △, 0.83; ▲, 0.9.

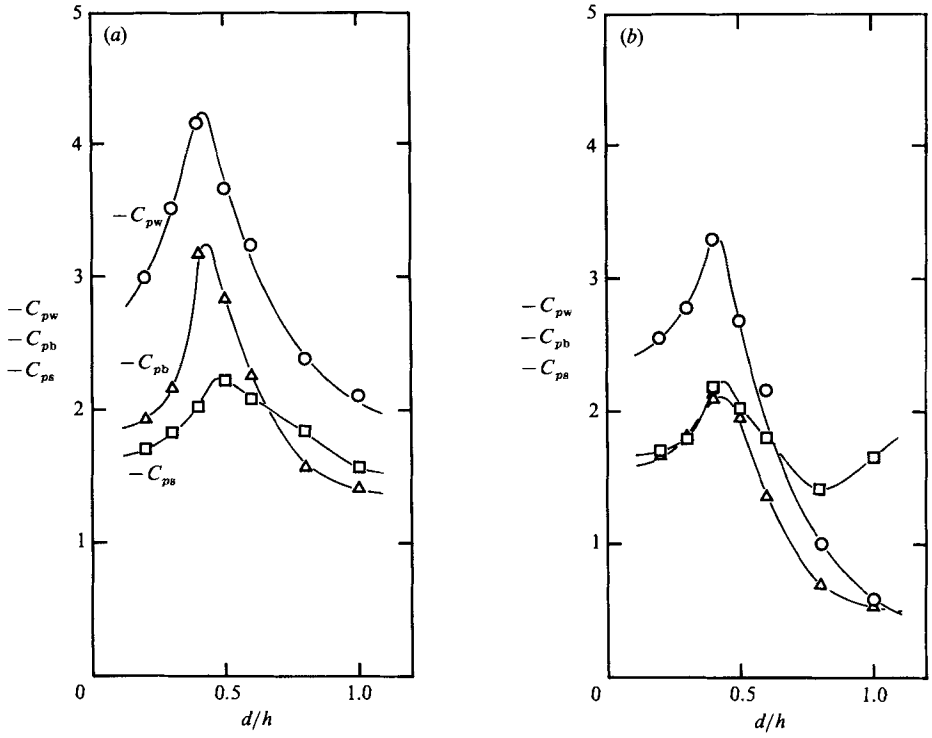

FIGURE 11. Variations of the base-pressure coefficient C_{pb}, the pressure coefficient at separation C_{ps} and the minimum pressure coefficient in the wake C_{pw} with d/h for oscillating rectangular cylinders. (*a*) $\bar{U} = \bar{U}_r$. (*b*) $\bar{U} = 3.9$.

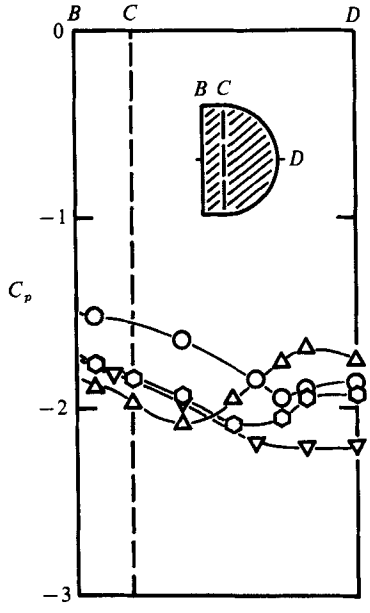

FIGURE 12. Pressure distributions around a D-section cylinder with $d/h = 0.7$ oscillating at low reduced velocities. ○, $\bar{U} = 6.7$; ▽, 5.8; ○, 5; △, 3.9.

weakened with a smaller pressure recovery ($\bar{U} = 5.0$), and eventually at the critical reduced velocity, $\bar{U} = 5.8$, the pressure distribution has a flat level over a region including the base. With further increase in $\bar{U}$ before reaching $\bar{U}_r$, the type of pressure distribution remains essentially unchanged but the level of pressures over the afterbody is increased ($\bar{U} = 6.7$).

For short rectangular cylinders oscillating at low reduced velocities below the critical, we also found that a reattachment-type pressure distribution is established on the side face. This is indicated in figure 11(*b*), where it can be seen that the gross pressure recovery $C_{pb} - C_{ps}$ at $\bar{U} = 3.9$ starts to increase at the critical depth. Another point of interest in figure 11(*b*) is that the variation of $-C_{ps}$ with d/h reverses its direction at $d/h = 0.8$, i.e. it now starts to increase with d/h. Bearman & Obasaju (1982) observed that at $\bar{U} = 4.0$ the flow around an oscillating square-section cylinder reattached intermittently to the side faces during part of the cycle. Thus, when intermittent reattachment occurs at low reduced velocities, natural vortex shedding behind the cylinder becomes less influential on the side-face flow so that $-C_{ps}$ now increases with the development of the shear-layer/edge direct interaction. The trend is more clearly seen in figure 5(*c*) for the square-section cylinder where $-C_{ps}$ increases rapidly with decreasing reduced velocity below $\bar{U} = 6.0$ while $-C_{pb}$ is progressively decreasing.

5.4. *Oscillating bluff cylinder with a fixed splitter plate*

With a spitter plate, the two shear layers issuing from a bluff cylinder cannot communicate with each other so that there is no formation of regular vortices behind the cylinder. In figure 13 the base-suction coefficient of an oscillating D-section cylinder with $d/h = 0.7$ with a fixed splitter plate is shown plotted against reduced velocity, whereas figure 14 shows pressure distributions on the same cylinder for several values of reduced velocity. The corresponding results for the cylinder without a splitter plate are also included for comparison in the two figures.

Figure 13 shows that there is a critical reduced velocity where base suction shows a peak, although it is only a mild one. The value of the critical reduced velocity, equal to about 6.0, is close to that for the cylinder without a splitter plate which is equal to 5.8. The experiment showed that the value of the critical reduced velocity was increased with increasing d/h. Figure 14 shows that a reattachment-type pressure distribution is established for reduced velocities lower than the critical for the cylinder with a splitter plate. It is interesting that the pressure distribution at a low reduced velocity of $\bar{U} = 3.9$ is similar to that for the cylinder without a splitter plate, although the mean level of pressure is different between the two. It thus appears that as the reduced velocity is lowered, the influence of the body oscillation on the mean flow tends to be separate from that of the natural vortex shedding.

The pressure distributions on the splitter plate are also interesting. We can see a large pressure recovery on the splitter plate for all reduced velocities shown. The wool-tuft test indicated that the flow did not reattach on the cylinder surface but reattached on the splitter plate. The pressure recovery at $\bar{U} = 3.9$ is thus twofold; one is caused by the shear-layer/edge direct interaction on the cylinder surface, and the other is caused by the final flow reattachment on the splitter plate.

5.5. *Base suction characteristics in the vortex-resonance range*

As can be seen in figure 5, the peak base suction at vortex resonance is lowered with increasing d/h beyond the critical, vanishes somewhere (figure 5*b*, *e*), and reappears as a mild one with further increase in d/h. It should be noted that the fluctuating lift

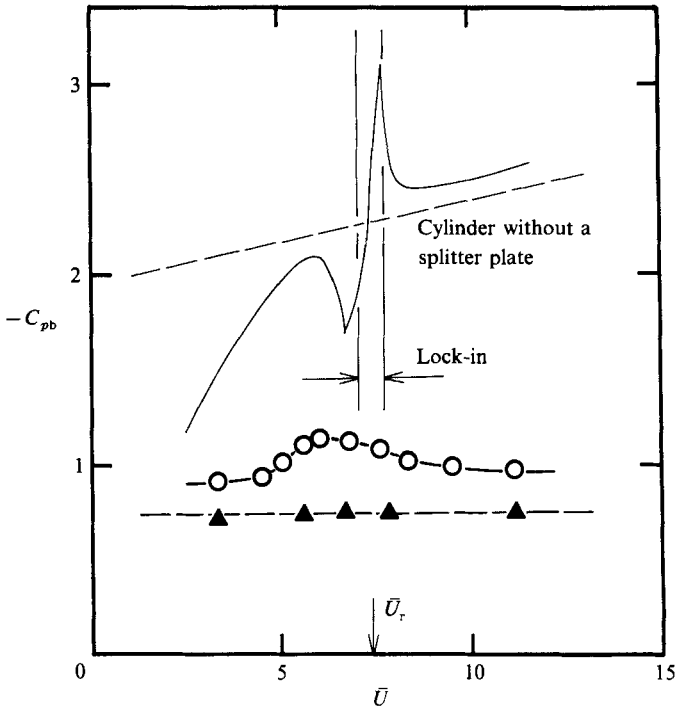

FIGURE 13. Base-suction coefficient versus reduced velocity for a D-section cylinder with $d/h = 0.7$ with a fixed splitter plate. Dashed line is for stationary cylinder.

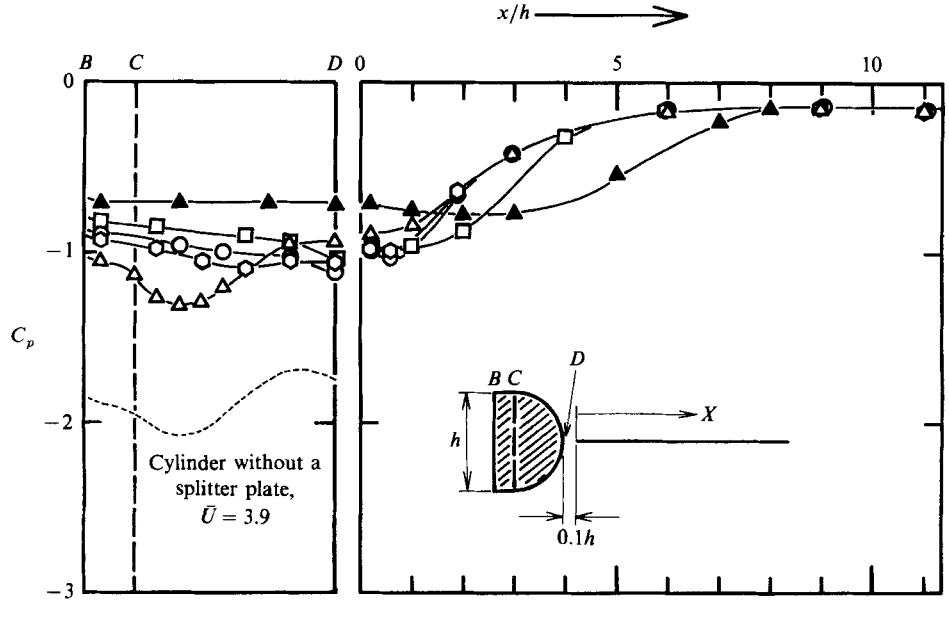

FIGURE 14. Pressure distributions around and behind a D-section cylinder with $d/h = 0.7$ with a fixed splitter plate. ▲, stationary; □, $\bar{U} = 8.9$; ○, 5.8; ⬡, 5; △, 3.9.

force of an oscillating rectangular cylinder with $d/h = 0.6$ shows a sharp peak at vortex resonance, although the (mean) base suction has no peak (Nakamura & Matsukawa 1987). Lowering of the base suction is certainly caused by the progressive development of the shear-layer/edge direct interaction. However, the mechanism by which a peak base suction reappears with further increase in d/h remains unclear. It might be because the flow would be closer to reattachment; if reattachment should occur, a peak base suction would appear at vortex resonance.

5.6. *Critical geometry of bluff bodies under various flow conditions*

There are many parameters that can influence the flow around a bluff body. These include, among others, the cross-section geometry, the incidence, the body oscillation and the free-stream turbulence. It has become apparent that critical geometry can be reached by controlling any one of them while keeping the others unaltered.

Bearman & Trueman (1972) showed that the value of the critical depth for rectangular cylinders can be sensibly controlled by changing incidence or using trailing-edge spoilers. Similar measurements were done by Nakamura & Tomonari (1977, 1979). It is well known (e.g. Laneville, Gartshore & Parkinson 1977; Nakamura & Tomonari 1976, 1981; Courchesne & Laneville 1982) that the free-stream turbulence can significantly lower the value of the critical depth of bluff cylinders such as rectangular and D-section ones. Most recently Naudasher (1987) discussed significant changes in the mean drags of circular and rectangular cylinders oscillating in the streamwise direction in connection with flow-induced in-line oscillations. It is important to mention that the most essential event common to all these cases is the manifestation of the shear-layer/edge direct interaction when critical geometry is reached.

6. Conclusions

The experiments on rectangular and D-section cylinders with variable afterbody lengths, forced to oscillate transversely over a wide range of reduced velocity including the vortex-resonance one, showed that the bluff-body mean flow was highly sensitive to body oscillation. The base-suction coefficient was strongly dependent both on the reduced velocity and on the afterbody length, but there was a close similarity in the base-suction characteristics between rectangular and D-section cylinders.

Just as bluff cylinders held stationary, oscillating bluff cylinders had a critical depth where a peak base suction was attained. The value of a critical depth was lowered with decreasing reduced velocity. An extraordinarily low critical depth with a very high suction was attained on cylinders oscillating at vortex resonance. For bluff cylinders with depths beyond the critical, a reattachment-type pressure distribution was established as a result of the shear-layer/edge direct interaction, thereby decreasing the base suction.

The experiment on an oscillating D-section cylinder with a fixed splitter plate showed that the shear-layer/edge direct interaction can also occur in this case. The reattachment-type pressure distributions on cylinders with and without a splitter plate at low reduced velocities were similar except for the mean level. It is therefore suggested that at low reduced velocities, the influence of the body oscillation on the mean flow can be separate from that of the natural vortex shedding. Finally, a remark is made on the critical geometry of bluff bodies under various flow conditions.

We thank Messrs K. Sugitani and K. Watanabe for technical assistance and Miss Y. Shinozaki for typing the manuscript.

REFERENCES

BEARMAN, P. W. 1984 Vortex shedding from oscillating bluff bodies. *Ann. Rev. Fluid Mech.* **16**, 195–222.

BEARMAN, P. W. & DAVIES, M. E. 1977 The flow around oscillating structures. *Proc. Fourth Intl Conf. Wind Effects on Buildings and Structures* (ed. K. J. Eaton), pp. 285–295. Cambridge University Press.

BEARMAN, P. W. & OBASAJU, E. D. 1982 An experimental study of pressure fluctuations on fixed and oscillating square-section cylinders. *J. Fluid Mech.* **119**, 297–321.

BEARMAN, P. W. & TRUEMAN, D. M. 1972 An investigation of the flow around rectangular cylinders. *Aero. Q.* **23**, 229–237.

COURCHESNE, J. & LANEVILLE, A. 1982 An experimental evaluation of drag coefficient for rectangular cylinders exposed to grid-turbulence. Trans. ASME I: *J. Fluids Engng* **104**, 523–528.

DA MATHA SANT'ANNA, F. A., LANEVILLE, A., TREPANIER, J. Y. & YONG, L. Z. 1987 Detailed pressure field measurements for some 2-D rectangular cylinders. *Prep. Seventh Intl Conf. Wind Engng, Aachen, July 6–10*, vol. 2, pp. 99–108, also *J. Wind Engng Indust. Aero.* **29** (1988), 241–250.

LANEVILLE, A., GARTSHORE, I. S. & PARKINSON, G. V. 1977 An explanation of some effects of turbulence on bluff bodies. *Proc. Fourth Intl Conf. Wind Effects on Buildings & Structures* (ed. K. J. Eaton) pp. 333–341. Cambridge University Press.

MIZOTA, T. 1984 An investigation of the unsteady aerodynamic characteristics of oscillating rectangular cylinders. Doctoral Thesis, Faculty of Engng, Kyushu University, Japan (in Japanese).

NAKAGUCHI, H., HASHIMOTO, K. & MUTO, S. 1968 An experimental study on aerodynamic drag of rectangular cylinders. *J. Japan Soc. Aero. Space Sci.* **16**, 1–5 (in Japanese).

NAKAMURA, Y. 1988 Recent research into bluff-body flutter. *Proc. Intl Coll. Bluff Body Aerodynamics and its Applications, Kyoto, October17–20*, pp. 1–10, also *J. Wind Engng* **37** (1988), 1–10.

NAKAMURA, Y. & MATSUKAWA, T. 1987 Vortex excitation of rectangular cylinders with a long side normal to the flow. *J. Fluid Mech.* **180**, 171–191.

NAKAMURA, Y. & MIZOTA, T. 1975 Unsteady lifts and wakes of oscillating rectangular prisms. *J. Engn Mech. Div. ASCE* **101** (EM6), 855–871.

NAKAMURA, Y. & OHYA, Y. 1984 The effects of turbulence on the mean flow past two-dimensional rectangular cylinders. *J. Fluid Mech.* **149**, 255–273.

NAKAMURA, Y. & OZONO, S. 1987 The effects of turbulence on a separated and reattaching flow. *J. Fluid Mech.* **178**, 477–490.

NAKAMURA, Y. & TOMONARI, Y. 1976 The effect of turbulence on the drags of rectangular prisms. *Trans. Japan Soc. Aero. Space Sci.* **19**, 81–86.

NAKAMURA, Y. & TOMONARI, Y. 1977 Galloping of rectangular prisms in a smooth and in a turbulent flow. *J. Sound Vib.* **52**, 233–241.

NAKAMURA, Y. & TOMONARI, Y. 1979 Pressure distributions on rectangular prisms at small incidence. *Trans. Japan Soc. Aero. Space Sci.* **21**, 205–213.

NAKAMURA, Y. & TOMONARI, Y. 1981 The aerodynamic characteristics of D-section prisms in a smooth and in a turbulent flow. *Aero. Q.* **32**, 153–168.

NAUDASCHER, R. 1987 Flow-induced streamwise vibrations of structures. *J. Fluids Struct.* **1**, 265–298.